SYNTHESIS, SPECTRAL ANALYSIS, QUANTUM CHEMICAL CALCULATION AND MOLECULAR DOCKING STUDIES OF INDOLE DERIVATIVE

Sulochana Devar[1]*, Vijayalaxmi Mallayya[2], Omnath Patil[3], Basavarajaiah S. M[4], Nagesh G. Y[5], S. M. Hanagodimath[6]

Abstract

The indole and its derivatives are privileged scaffold in drug discovery as well as development. We herein report the theoretical and experimental study of ethyl 5-methyl-3-phenyl-1*H*-indole-2-carboxylate (5-MPIC). The solvatochromic shift method is utilized for studying the solvents' imapct on 5-MPIC. Molecule's emission as well as absorption spectra were obtained at room temperature (300K) in alcohol. Bakshiev, Lippert, as well as Kawaski Chamma Viallets equations have been used to produce experimental estimates for the dipole moments in the excited along with ground states. When compared to the dipole moments of the ground state, those of the excited state are bigger, proving that the excited state is more polar. The Catalan and Kamlet-Taft equations are used in the calculation of the linear solvation energy relation. We used the Gaussian 16W programme with the B3LYP 6-31+G (d, p) basis set for determining optimal molecular shape, Mulliken, NLO, HOMO-LUMO, NBO, and atomic charges. This molecule's physicochemical features, including its drug-likeness as well as bioactivity, have been determined. To learn about the compound's biophysical characteristics, molecular docking experiments were conducted using cyclooxygenase-2 (PDB ID-Cox-2).

Keywords: Indole; DFT; Kamlet Taft; Catalan; Molecular docking; Solvatochromic shift.

[1]*,[2],[3],[6]Department of PG "Studies and Research in Physics, Gulbarga University, Kalaburagi-585 106, Karnataka-India

[4]PG Department of Chemistry, Vijaya College, R. V. Road, Bengaluru-560004, Karnataka, India"

[5]Department of Chemistry, Guru Nanak First Grade College, Bidar, Karnataka, India

*Corresponding Author: Sulochana Devar

*Department of PG "Studies and Research in Physics, Gulbarga University, Kalaburagi-585 106, Karnataka-India

Eur. Chem. Bull. **2023**, *12(Special Issue 5), 6704 - 6717*

6704

1.Introduction

Researchers in the field of quantum chemistry greatly benefit from experimentally obtained data on the electro-optical properties of molecules in various states, which may be used to compare with theoretical records or to evaluate certain computational procedures based on the data. The digital valence cloud, which is particularly sensitive to external influences, may be found in the fluorescence and absorption spectra of electronic states.

Solute molecules in a solution are affected by the internal electrostatic field generated by the solvent molecules [1]. The electro-optical characteristics of the spectrally active molecules and magnitude of internal reactive field influence the strength of solvent-solute interactions [2]. In most cases, the transition and absorption occur between electronic states that have differing molecular characteristics. Hence, the dissimilarity between the solute and solvent solvation energies [3-5].

Effective dye-sensitized solar cells [6] may be made using indole-based chemicals, which also have many other uses in the biological sciences [7-8]. ant hypersensitizing, antispasmodic, anti-inflammatory, antifungal, antibacterial, anticancer effects were all seen in indole as well as its derivatives [9]. There are numerous research articles [10-15] in the literature describing indole derivative studies, particularly the solvatochromic method. This is a standard approach of determining a molecule's dipole moment. This technique depends on a linear connection between the absorption and emission wavenumbers as well as the solvents' polarity functions. Because computational tools can assess specific molecular properties fast and correctly, Researchers are keen in theoretical studies that might validate their empirical findings.

An appropriate quantum chemical study can aid in the economically predicted properties of a compound as well as the clarification of some experimental phenomena [16-19]. This allows for theoretical research to be utilised to provide numerical estimates for experimental results. In this case, we used DFT (density functional theory) as well as molecular docking to investigate the 5-MPIC molecule. From the literature, we find that no such work has been done on this class of molecules. To understand this class of molecules, this work was performed and reported.

2.Experimental

2.1. Materials and method

5-MPIC, an indole derivative, was produced by following the specified procedure [20-22]. Decanol, Methanol, Nonanol, Ethanol, Octanol, Butanol, Heptanol, Pentanol, Hexanol, Propanol, were the solvents used in this study, and they all belonged to the spectroscopic grade. There was no further refining of the solvents before they were used. The required solution has been ready with solute concentration that was held constant at 1×10^{-6}M. The solvent concentration was kept low enough to minimise the impact of self-absorption.

With a twin beam PG Insta Ltd. model T-90+ UV-V spectrophotometer, we were able to note the 5-MPIC's absorption as well as fluorescence spectra in diverse solvents from 250 to 550 nm wavelength at room temperature. Hitachi F-2700 fluorescence spectrophotometer has been used to get the spectra of fluorescence. The Origin software has been used to analyse the data.

Quantum chemical calculations were executed for extracting the ground state dipole moment, HOMO-LUMO, Mulliken atomic charges, NLO (Nonlinear optical properties) and NBO (Natural orbital bonding) properties. The calculations have been performed utilizing GAUSSIAN -16W program at photophysical laboratory, Department of Physics, Gulbarga University, Kalaburagi.

Scheme 1: Synthesis of ethyl 5-methyl-3-phenyl-1*H*-indole-2-carboxylate
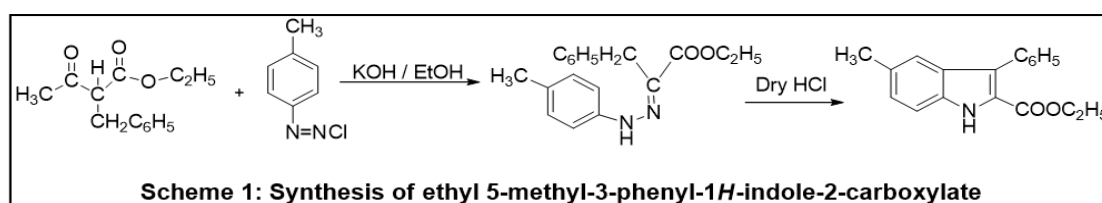
3. Theoretical background

3.1. Estimation of ground state and excited state dipole moments using the Solvatochromic shift method

Several techniques, such as solvatochromic, electronic and, thermochromic, may be utilized for calculating the natural compounds' excited along with ground state dipole moments. The solvatochromic technique was selected because it provides reliable findings for a large variety of chemicals. Three separate equations have been

Eur. Chem. Bull. **2023**, *12(Special Issue 5), 6704 - 6717*

6705

employed to approximate the 5-MPIC molecule's dipole moments in both its excited and ground states: Lippert's equation, [23]

$$\overline{v}_a - \overline{v}_f = m_1 F_1(\varepsilon, n) + \text{Constant} \tag{1}$$

Baksheiv's equation, [24]

$$v_a - \overline{v}_f = m_2 F_2(\varepsilon, n) + \text{Constant} \tag{2}$$

Kawaski Chamma Vialette's equation, [25, 26]

$$\frac{\overline{v_a} + \overline{v_f}}{2} = m_3 F_3(\varepsilon, n) + \text{Constant} \tag{3}$$

The polarity parameters of the solvents are denoted by the symbols F1, F2, and F3, respectively.

$$F_1(\varepsilon, n) = \left[\left(\frac{(\varepsilon-1)}{2\varepsilon-1}\right) - \frac{(n^2-1)}{(2n^2-1)}\right] \tag{4}$$

$$F_2(\varepsilon, n) = \left[\frac{(2n^2-1)}{(n^2+2)}\right]\left[\left(\frac{\varepsilon-1}{\varepsilon+2}\right) - \left(\frac{n^2-1}{n^2+2}\right)\right] \tag{5}$$

$$F_3(\varepsilon,n) = \left\{\frac{1}{2}\frac{(2n^2+1)}{(n^2+2)}\left[\frac{\varepsilon-1}{\varepsilon+2} - \frac{n^2-1}{n^2+2}\right] + \frac{3}{2}\left[\frac{n^4-1}{(n^2+2)^2}\right]\right\} \tag{6}$$

where, $\overline{v}_f$ and $\overline{v}_a$ are defined as the maxima wavenumber of fluorescence and absorption in cm^{-1}, respectively. 'ε' is defined as dielectric constant 'n' is defined as refractive index. From (4) (5) and (6) equations, graphs $(\overline{v}_a - \overline{v}_f)$ *v/s* $F_1(\varepsilon, n)$, $(\overline{v}_a - \overline{v}_f)$ *v/s* $F_2(\varepsilon, n)$ and $\frac{\overline{v_a}+\overline{v_f}}{2}$ *v/s* $F_3(\varepsilon, n)$ were plotted respectively where m_1, m_2, and m_3 slopes are obtained respectively, as shown below.

$$m_1 = \frac{2(\mu_e - \mu_g)^2}{hca^3} \tag{7}$$

$$m_2 = \frac{2(\mu_e - \mu_g)^2}{hca^3} \tag{8}$$

$$m_3 = \frac{2(\mu_e^2 - \mu_g^2)}{hca^3} \tag{9}$$

Where μ_e is defined as the ground state' molecules dipole moments, μ_g is defined as the molecules' dipole moments of excited state. Planck constant is defined by symbol '**h**' whereas velocity of light in vacuum is defined by symbol '**c**', Onsager's cavity radius is defined by symbol '**a**'. Atomic increment technique, introduced by Edward Lorenz, is used to determine the value of **a**. [27]. The equations (10) and (11) are obtained on the basis of equations (8) and (9).

$$\mu_g = \frac{m_3 - m_2}{2}\left[\frac{hca^3}{2m_2}\right]^{\frac{1}{2}} \quad \text{For}(m_3 > m_2) \tag{10}$$

$$\mu_e = \frac{m_3 + m_2}{2}\left[\frac{hca^3}{2m_2}\right]^{\frac{1}{2}} \tag{11}$$

3.2 Molecular microscopic solvent polarity parameter

The molecular microscope, E_T^N solvent polarity function introduced by Reichardt [28] may be used to learn about the polarisation dependency or the impact of hydrogen bonding on certain features. Reichardt proposed, and Ravi developed, the theoretical foundation for the Stokes shift connection with, E_T^N. Based on this, we may write (12) where, E_T^N is the resulting expression.

$$E_T^N = \frac{E_T(Solvent) - 30.7}{32.4} \tag{12}$$

The pyridinium-N-phenolate betaine dye has an intramolecular charge transfer absorption peak at a red wavelength of $E_T(Solvent) = 28,591/\lambda_{max}$. Here, we use stokes shift vs., E_T^N graphs to determine the resulting change in dipole moment.

$$\overline{v_a} - \overline{v_f} = 11307.6\left(\frac{\Delta\mu^2 a_D^3}{\Delta\mu_D^2 a^3}\right)E_T^N + \text{Constant} \tag{13}$$

In the above equation, $\Delta\mu = (\mu_e - \mu_g)$ is defined as the change in the dipole moment whereas 'a' is indole molecule's Onsager cavity radius. Since we know aD and D values (6.2 and 9D), we can use this information to insert a ratio using the Onsager radii of Betadine dye and an indole derivative into the formula.

3.3. Correlation with multiparameter solvent polarity scale

Numerous physical and chemical aspects involving solute-solvent interactions may be correlated with the help of solvatochromic parameters. There are many polarity scales for these factors. Two well-known multiparametric weights are optimal for quantifying the nature of the various solvent-specific interactions: the Kamlet-Taft [29, 30] and Catalan solvatochromic approaches [31, 32] or LSER (linear solvation energy relations).

Predicting different photophysical properties in different sorts of solution equilibria can be done with the help of the Kamlet-Taft and Catalan empirical solvation scales, which take into account the solvent's polarity, SPP/p* (polarizability), SB /b (basicity) and SA /a (acidity) by measuring the specific interactions occurring locally in the

Eur. Chem. Bull. **2023**, *12(Special Issue 5), 6704 - 6717*

6706

solution shell. Kamlet-Taft (Eq. 14) and Catalan (Eq. 15) expressions are given as:

$$y = y_0 + a\alpha + b\beta + c\pi^* \tag{14}$$

$$y = y_{0 +}a_{SA}SA_+ b_{SB}SB + c_{SP}SP + d_{SdP}SdP \tag{15}$$

Absolute ion characteristics are represented by s*/SSPP, a/aSA, and b/bSB. s*/SSPP characterise the solute's polarizability/polarity, a/aSA defines the solute's propensity to absorb hydrogen bonds from the solvent, and b/bSB quantifies the solute's propensity to emit hydrogen bonds to the solvent. Parameters for numerous solvents are included in Table 3, which was compiled using references [33, 34].

3.4 Molecular docking studies
3.4.1. Preparation of protein and ligand structure for docking studies
Cyclooxygenase-2 coordinates were obtained from the protein database [35]. Redocking with 6COX has been utilized to determine the binding affinity of the crystallised ligand 1-phenylsulforamide-3-trifluoromethyl1-5-prabromophrnylpyrazole S58). The docking studies were carried out using the Auto Dock programme (version 4.2.3), a successful protein-ligand binding prediction tool [36]. Open Babel was used in PyRx0.9.9 [37] to minimise energy. Since the protein is a homodimer by nature, only the chain was taken into account for the docking study. The x, y, and z coordinates of the docking region for 6COX were set for interaction with the target protein and were centred at 27.77, 29.38, and 40.14 respectively. The docking region was defined using Auto Grid with a grid box size of 201 x 258 x 219 and a grid spacing of 0.375. We conducted 10 independent docking runs with 150 randomly distributed individual sets for each docked compound. Using Lamarck's genetic algorithm, 250000 energy evaluations were performed for each docking calculation. A graphical user interface for docking studies called PyRx 0.99 was employed. Specifics of protein-ligand interactions were analysed with the help of the Protein-Ligand Interaction Profiler [38].

4.RESULTS AND DISCUSSION
4.1. Solvent effects on absorption and fluorescence emission spectra
5-MPIC's emission and absorption spectra in numerous solvents are presented in Figures 2, 3. Absorption peaks may be seen between 310 nm and 350 nm. The fluorescence spectra exhibit a maximum at around 390–415 nm. Table 1 represents the wavenumbers, Stokes shifts and arithmetic mean shifts for the molecule in various solvents. There is a significant difference in Stokes shift of around 8236 cm-1 [39], with 4411cm^{-1} to 12647cm^{-1} range in magnitude. Tables 1 along with 2 demonstrate that Stokes shift undergoes a bathochromic shift whenever the polarity of the solvent is increased, presenting more support to the existence of the $\pi \rightarrow \pi^*$ transition. As can be seen in Table 12, the dipole moment of the excited state is greater than that of the ground state.

The linear Lippert polarity function, Bakshiv polarity function, along with Kawasaki chamma polarity violet polarity function vs Stokes shift are presented in Figures 4, 5, and 6. The Stokes shift has been utilised to probe the shift in the dipole moment (see Figure 7) as a function of the, E_T^N parameter (see Figure 6). The slope is utilized for calculating μ_g and μ_e. Table 11 **listed** the dipole moment, radius, datapoints, correlation factors, slopes and change in the dipole moment of 5-MPIC.
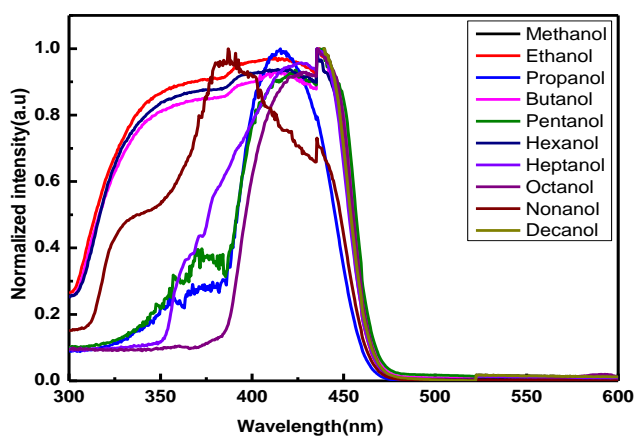
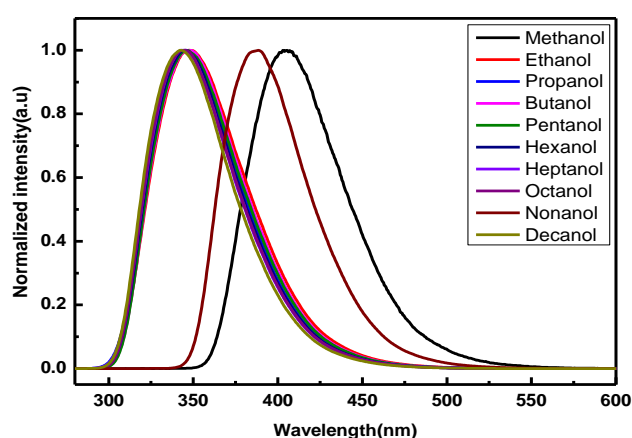**Figure 2:** Normalised absorption spectra 5-MPIC
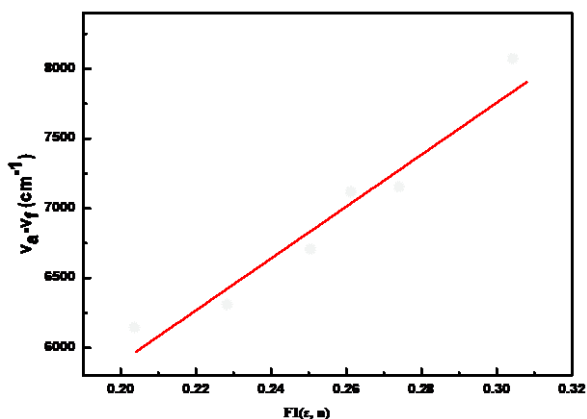
Figure 3: Normalized fluorescence of 5-MPIC

Eur. Chem. Bull. **2023**, *12(Special Issue 5), 6704 - 6717*

6707

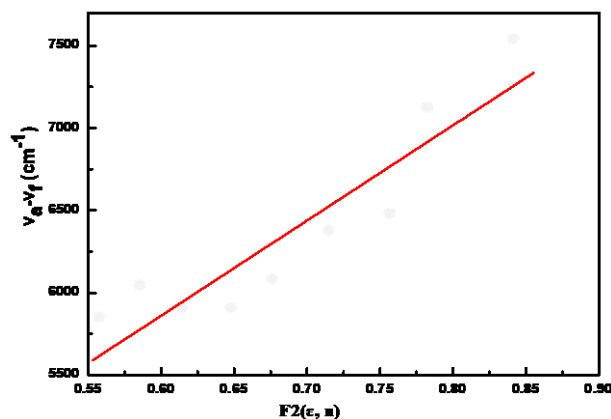**Figure 4:** Lippert's polarity function 5-MPIC

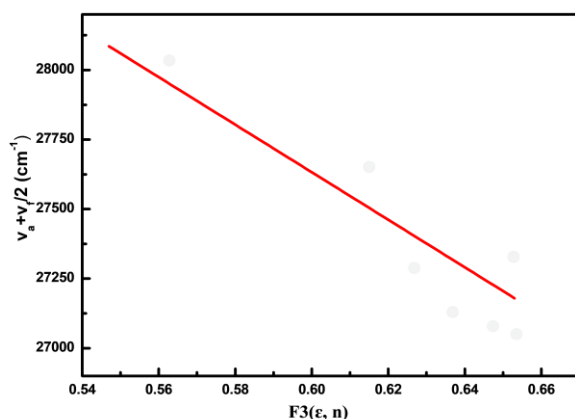**Figure 5:** Baksheive's polarity for function for 5-MPIC

Figure 8: Kawaski Chamma Viallets polarity function
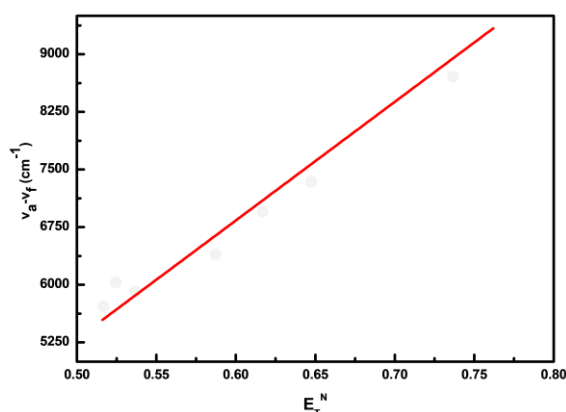polarity function for 5-MPIC

Figure 7: "Variation of stoke shift with E_T^N
for 5-MPIC

Table 1: Absorption maxima, fluorescence maxima wave number, Stokes shift and arithmetic stokes shift
data

Solvents	$\overline{\nu_a}$ cm^{-1}	$\overline{\nu_f}$ cm^{-1}	$\overline{\nu_a} - \overline{\nu_f}$ cm^{-1}	$\dfrac{\overline{\nu_a} + \overline{\nu_f}}{2}$ cm^{-1}
Methanol	37037	24390	12647	30713
Ethanol	29411	24390	5021	26900
Propanol	31250	24350	6900	27800
Butanol	28985	24096	4889	26540
Pentanol	29850	24096	5754	26973
Hexanol	29411	25000	4411	27205
Heptanol	30303	25000	5303	27651
Octanol	30303	24390	5913	27346
Nonanal	35714	24096	11618	29905
Decanol	30303	24096	6207	28751

Table 2: Polarity function and microscopic solvent polarity parameter for respective solvents

Solvents	ε	n	F1(ε, n)	F2(ε, n)	F3(ε, n)	E_T^N
Methanol	33.0	1.329	0.308	0.855	0.652	0.762
Ethanol	24.6	1.360	0.289	0.830	0.652	0.654
Propanol	20.6	1.387	0.274	0.781	0.653	0.617
Butanol	17.4	1.399	0.263	0.749	0.646	0.586
Pentanol	14.8	1.409	0.253	0.716	0.636	0.568
Hexanol	13.0	1.417	0.244	0.686	0.626	0.559
Heptanol	11.3	1.428	0.232	0.650	0.615	0.549
Octanol	9.80	1.428	0.223	0.614	0.547	0.537
Nonanal	9.00	1.430	0.216	0.590	0.587	0.528
Decanol"	8.00	1.437	0.204	0.553	0.573	0.525

4.2 Multiple linear regression analysis

Analysis utilizing Kamlet-Taft and Catalan's proposed Multiple Regression (MLR) technique. Bathochromic variations in fluorescence and absorption spectra with rising polarity are attributable to negative values of all parameters in Eqs. (14) and (15), as proven by the Kamlet-Taft and Catalan solvent scale (15).

Kamlet-Taft parameter

$\overline{v}_a = 56052 + 5028\alpha - 26837\beta + 2601\ \pi^*$

$\Delta\overline{v} = 15840 - 6744\alpha - 12746\beta + 14417\pi^*$

The solvent in the molecule of interest is significantly affected by the non-specific dielectric interaction (π^*) as seen in preceding equation. But HBA and HBD parameters value can't be underestimated. Multiple regression analysis of $\overline{v}a$

and $\Delta\overline{v}$ shows that HBA (β) has more influence than HBD (α). This suggests that the spectroscopic features of these molecules are not as dependent on solvent's hydrogen bonding. More so, the solvatochromic characteristics of SdP, SP, SB, and SA, are linked to the spectroscopic properties of $\Delta\overline{v}$ and $\overline{v}a$ molecules:

$\overline{v}_a = 320045 + 21245\ SA + 92940\ SB + 568393\ SP + 54352\ SdP$

$\Delta\overline{v} = 90942 - 7274\ SA + 21106\ SB + 75614\ SP - 21563\ SdP$

According to the above equation, solvent has a greater influence on polarizability (SP) and dipolarizability (SdP). Conversely, acidic and basic solvent effects should be considered. A solvent's basicity (SB) is greater than its acidity (SA) [40].

Table 3: The values of Kamlet solvatochromic parameters and Catalan emphatical solvents scale SA, SB, SP, SdP in alcohols

Solvents	α	β	π^*	SA	SB	SP	SdP
Methanol	0.98	0.66	0.60	0.605	0.545	0.608	0.904
Ethanol	0.86	0.75	0.54	0.400	0.658	0.633	0.783
Propanol	0.84	0.90	0.52	0.367	0.782	0.658	0.748
Butanol	0.84	0.84	0.47	0.341	0.809	0.674	0.655
Pentanol	0.84	0.86	0.40	0.319	0.86	0.687	0.587
Hexanol	0.80	0.86	0.40	0.315	0.879	0.698	0.552
Heptanol	0.80	0.86	0.40	0.302	0.912	0.706	0.499
Octanol	0.77	0.81	0.40	0.299	0.923	0.713	0.454
Nonanal	0.70	0.80	0.40	0.270	0.906	0.717	0.429
Decanol	0.70	0.82	0.45	0.259	0.912	0.722	0.383

4.2 Analysis of quantum chemical calculation
4.2.1 Optimised structure

Optimal molecular geometry was calculated utilizing DFT/B3LYP process with 6-31+G (d, p) basis set over Gaussian 16W as given in Fig 8.. There is a theoretically predicted dipole moment of 0.88 D for the 5-MPIC compound, which corresponds to the direction of dipole moment. Taking into consideration the chemical's interaction with the molecules of the solvent is necessary for obtaining correct values for the dipole moments in both the ground as well as excited energy states.
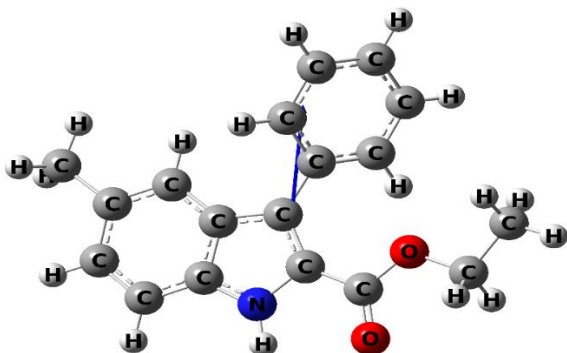

Figure 8: Optimized structure of 5-MPIC

4.2.2. Frontier molecular orbital analysis

The molecule's chemical reactivity as well as stability may be defined in part by its GCRD (Global Chemical Reactivity Descriptors). Chemical Potential, IP (ionisation potential), electron negativity (χ), chemical softness, EA (electron affinity), chemical hardness (η), of molecule in ethanol and gas phase are represented in Table 4. This reveals that all values in the solvent are greater than in the gas phase. 5-MPIC is highly reactive according to the IP and EA values [41]. 5-MPIC is electronegative due to the carbonyl oxygen because electronegativity describes a molecule's ability for attracting electron density. The fact that 'µ' is negative also indicates that 5-MPIC is highly reactive. In addition, this frontier molecular orbital calculation utilizing DFT /B3LYP with 6-31+G (d, p) as the basis set reveals that 5-MPIC is moderately stable and readily polarizable due to its low chemical hardness, energy gap, as well as chemical softness. Figure 9 depicts the 3D HOMO-LUMO plots in vacuum and ethanol.

Table 4: HOMO-LUMO Energy gap

Parameters (in ev)	In gas phase	In ethanol
HOMO	-0.2044	-0.2103
LUMO	-0.0536	-0.0612
IP =-HOMO	0.2044	0.2103
EA)= -LUMO	0.0536	0.0612
$\chi = \dfrac{IP + EA}{2}$	0.1290	0.1358
$\mu = -\chi$	-0.1290	-0.1358
$\eta = \dfrac{IP - EA}{2}$	0.0754	0.0745
$s = 1/2\eta$	6.6304	6.7073
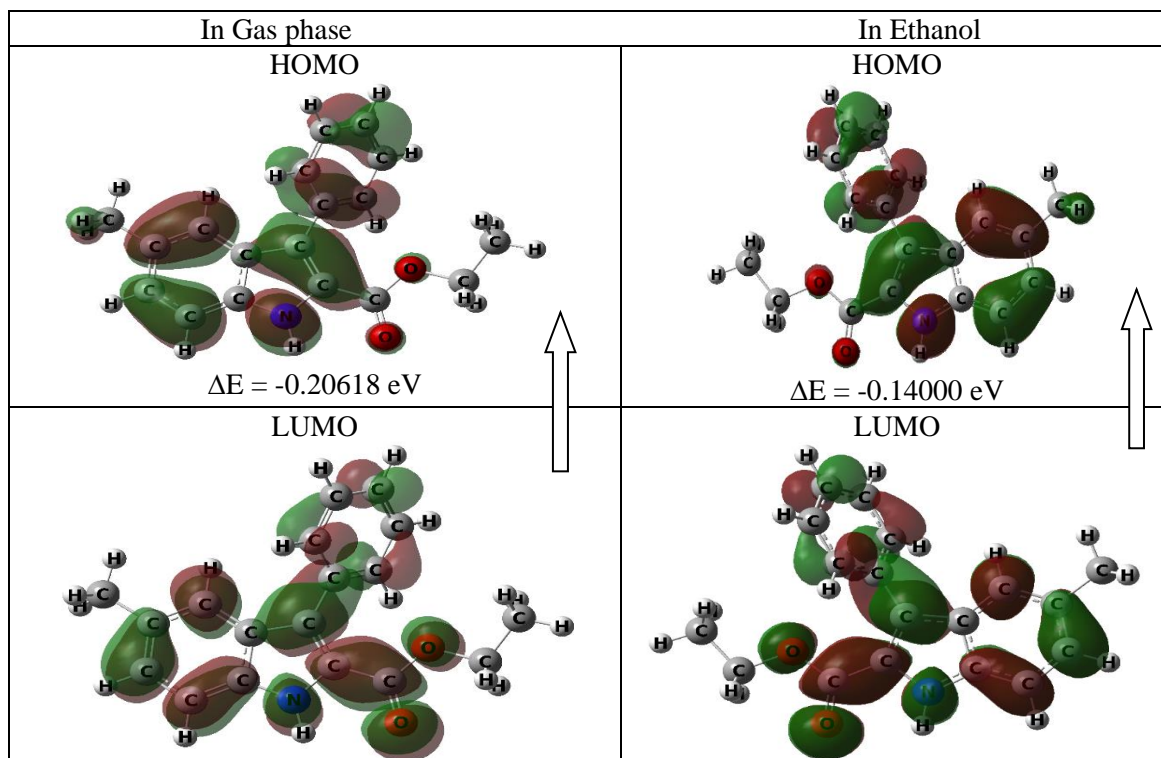
Figure 9: HOMO-LUMO Energy gap

4.2.3 Mulliken atomic charges

The idea of atomic charge as well as transfer of charge between atoms is the basis for understanding molecular behaviour and reactivity. Hence, the study of atomic charges is crucial in quantum chemistry. Atomic charges are determined utilizing DFT/B3LYP process and G (d, p) +6-31 basis set for analysing Mulliken population [42]. Figure 10 depicts the Mulliken charges, and Table 5 lists the value

Figure 10: Mulliken atomic charges

Eur. Chem. Bull. **2023**, *12(Special Issue 5), 6704 - 6717*

6710

Table 5: Mulliken atomic charges

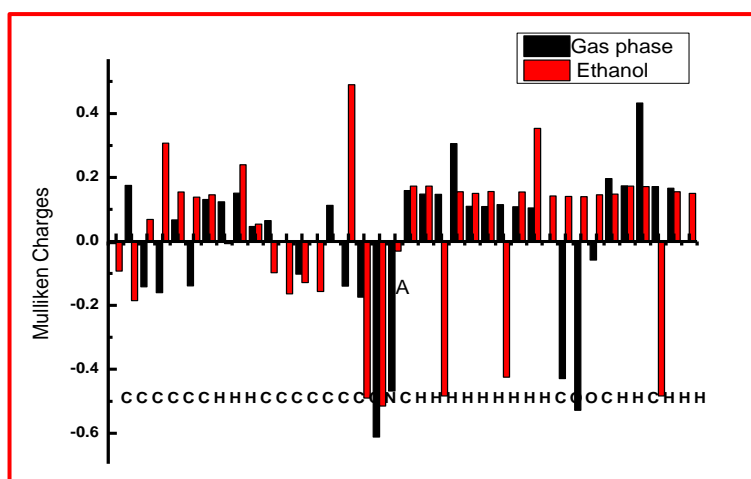| S.No.	Atom	Charge value (Gas phase)	Charge value (Ethanol)
1	C	-0.007	-0.093
2	C	0.175	-0.186
3	C	-0.142	0.069
4	C	-0.161	0.307
5	C	0.067	0.154
6	C	-0.139	0.138
7	H	0.131	0.145
8	H	0.124	-0.007
9	H	0.151	0.240
10	C	0.047	0.054
11	C	0.065	-0.098
12	C	-0.154	-0.164
13	C	-0.103	-0.129
14	C	-0.122	-0.157
15	C	0.113	-0.141
16	C	-0.140	0.490
17	C	-0.174	-0.490
18	N	-0.612	-0.515
19	C	-0.468	-0.031
20	H	0.159	0.173
21	H	0.148	0.173
22	H	0.147	0.484
23	H	0.306	0.156
24	H	0.110	0.150
25	H	0.109	0.156
26	H	0.115	-0.424
27	H	0.108	0.155
28	H	0.105	0.354
29	C	0.429	0.142
30	O	0.429	0.141
31	O	-0.528	0.140
32	C	-0.058	0.146
33	H	0.196	0.148
34	H	0.173	0.173
35	C	0.433	0.172
36	H	0.171	-0.484
37	H	0.166	0.156
38	H	0.152	0.150

4.2.4. Natural Bond Orbital Analysis

NBO analysis calculated with Gaussian 16w software can be used to efficiently analyze intra- and intermolecular bonding, providing an auxiliary mode for studying charge transfer or hyperconjugated interactions, rehybridization, intramolecular charge delocalization, and electron affinity within molecules [43]. The NBO approach, which expresses the perturbation energy E, is used to quantify the binding and anti-binding interactions caused by the second-order perturbations E (2).

$$E\ (2) = \Delta E_{ij} = q_i \frac{(Fij)^2}{(Ej - Ei)}$$

Here, diagonal elements are represented by Ei and Ej, donor orbital's occupation is represented by qi and off-diagonal NBO matrix elements is represented by Fij. Table 6 displays the results of a calculation of productive interactions between an occupied Lewis-type NBO orbital (bonding) and antibonding. There are two kinds of donors as well as acceptors, denoted by π and σ and, π* and σ*. Based on measurements of the transition's dispersion energy E2, we can deduce its probability for the following states: C1-C2 C3-C4 (17.48KJ/mol π π*), C3-C4→C1-C2 (19.06KJ/mol π→π*), C5-C→6C3-C4 (19.5KJ/mol ππ*), C10-C11→C29-O30 (26.93KJ/mol π→π*. This transition is indicative of a significant role played by π-electrons, that engage in substantial hyper conjugative interactions between molecules. The

high polarizability is due to the NLO activity of the molecule, that is in turn due to the strong intermolecular contacts created by orbital overlap of the $\pi \rightarrow \pi^*$ transition indicated by the NBO study [44].

4.2.5 Nonlinear optical properties

Electron motion along the molecule's length is linked to its nonlinear optical characteristics. Increasing the degree of conjugation enhances the molecule's nonlinear optical characteristics. Nonlinear optical characteristics may also be enhanced by the addition of strong acceptor and donor groups. Elevated temperatures increase both the main hyperpolarizability and polarizability of organic molecules, as well as the electron superposition on them. [45]. The results of the DFT/B3LYP calculation of the β_0 (first polarizability), $\Delta\alpha$ (polarizability anisotropy), α (polarizability), μ (Dipole moment) of the indole molecule are presented in Table 7.

4.2.6 Molecular docking studies

Molecular docking investigations' results of using AutoDock4.2 software are shown in Table 8. The protein 6-COX was docked with the 5-MPIC. To understand the intermolecular interactions, the results are compared to the reference molecule S58. The most stable cluster size and the lowest binding energy for every protein's active site conformation were selected for the interaction investigations. S58, the reference ligand, is a diaryl heterocyclic inhibitor that is selective for COX -2 over COX -1. The inhibition constant was calculated to be 462.11 nM, and binding affinity has been determined to be -8.64kcal/mol. The co-crystallized inhibitor (S58) formed three hydrogen bonds with ASN39, CYS47, and TYR130.The ligand methyl indole interacted at a new binding pocket created by conformational changes at Tyr355, which opened a hydrophobic pocket composed of Leu352, Ser353, Tyr355, Phe518 and Val523, as well as the formation of a salt bridge with Arg120. Binding energy was -7.93 kcal/mol for methyl indole, while the inhibition constant was 1.54 M, making it the most potent of all the compounds tested. Using the hydrogen-bonding interaction diagram, Figure 11 shows how the ligand in the stick interacts with the amino acids.

"Table 6: Second order perturbation theory analysis of Fock matrix in NBO basis for 5-MPIC

Donor (i)	Occupancy	Acceptor(j)	Occupancy	E2 (Kj/ mol) [a]	E(j)-E(i) (a.u) [b]	F(i,j)(a.u) [c]
π (C1-C2)	1.5755	π^*(C3-C4)	0.2995	17.48	0.27	0.064
π (C3-C4	1.9759	π^*(C1-C2)	0.0275	19.06	0.29	0.069
π (C5-C6)	1.9748	π^*(C3-C4)	0.2995	19.50	0.27	0.069
π (C10-C11)	1.9694	π^*(C29-O30)	0.0198	26.93	0.23	0.073
σ (C1-C10)	1.9617	σ^*(C2-C3)	0.0228	2.15	1.18	0.045
σ (C2-C3)	1.9757	σ^*(C2-N18)	0.0241	4.11	1.23	0.045
σ (C2-N18)	1.9759	σ^*(C3-C4)	0.2995	1.02	1.12	0.030
σ (C3-C4)	1.9985	σ^*(C3-H7)	0.1277	2.76	1.16	0.048
π (C3-C4)	1.7493	σ^*(C4-C5)	0.2368	0.90	1.06	0.002
σ (C3-H7)	1.9714	σ^*(C4-H8)	0.0115	1.37	1.16	0.036
σ (C4-C5)	1.9755	σ^*(C5-C6)	0.0202	2.96	1.24	0.054
σ (C4-H8)	1.9981	σ^*(C5-C19)	0.0152	2.23	1.17	0.046
σ (C5-C6)	1.7242	σ^*(C10-C11)	0.3713	3.33	1.28	0.058
π (C5-C6)	1.9748	σ^*(C10-C15)	0.0292	18.14	0.28	0.066
σ (C5-C19)	1.9831	σ^*(C11-N18)	0.0196	2.29	1.12	0.030
σ (C6-H9)	1.9779	σ^*(C12-C13)	0.0154	1.38	1.15	0.036
π (C10-C11)	1.9694	π^*(C13-C15)	0.3608	0.84	1.26	0.029
σ (C10-C15)	1.9710	σ^*(C13-C27)	0.0120	2.74	1.13	0.050
σ (C11-N18)	1.9800	σ^*(C14-C16)	0.0165	1.10	1.07	0.031
σ (C11-C29)	1.9792	σ^*(C14-H24)	0.0121	0.88	1.25	0.030
σ (C12-C13)	1.9760	π^*(C16-C17)	0.0248	2.O3	1.23	0.045
π (C12-C14)	1.9803	σ^*(16-H25)	0.0121	2.78	1.26	0.053
σ (C12-C26)	1.9826	σ^*(C17-H28)	0.0185	1.32	1.16	0.035
π (C13-C15)	1.9712	π^*(N18-H23)	0.0188	3.14	1.25	0.056
σ (C13-C27)	1.9982	σ^*(C19-H20)	0.0088	1.43	1.16	0.036
σ (C14-C16)	1.9980	σ^*(C19-H21)	0.0041	2.65	1.26	0.052
σ (C15-C17)	1.9714	π^*(C29-O30)	0.0198	2.89	1.22	0.053
σ (C17-C28)	1.9981	σ(C32-H33)	0.0181	2.12	1.16	0.044
σ (N18-H23)	1.9989	σ^*(C32-H34)	0.0179	0.92	1.24	0.030
σ (C19-H20)	1.9823	σ^*(C35-H36)	0.0075	2.65	0.67	0.066

Eur. Chem. Bull. **2023**, *12(Special Issue 5), 6704 - 6717*

6712

Table 7: Electric dipole moment, polarizability and first hyper polarizability of 5-MPIC"

Parameters	(esu)*10^{-33}
α_{xx}	-95.54
α_{yy}	-123.29
α_{zz}	-127.92
α_{xy}	0.40
α_{xz}	-3.50
α_{yz}	-2.66
α_0	-115.58
$\Delta\alpha_0$	30.96
β_{xxx}	48.93
β_{yyy}	21.93
β_{zzz}	4.70
β_{xyy}	-27.89
β_{xxy}	-17.63
β_{xxz}	0.95
β_{xzz}	12.39
β_{yzz}	-12.13
β_{yyz}	10.89
β_{xyz}	6.64
β_0	34.28
μ_x	-0.14
$\mu(D)$	0.88
μz	0.79
μ_y	0.44

Table 8: Molecular interaction of 5-MPIC and reference inhibitor S58 with 6COX

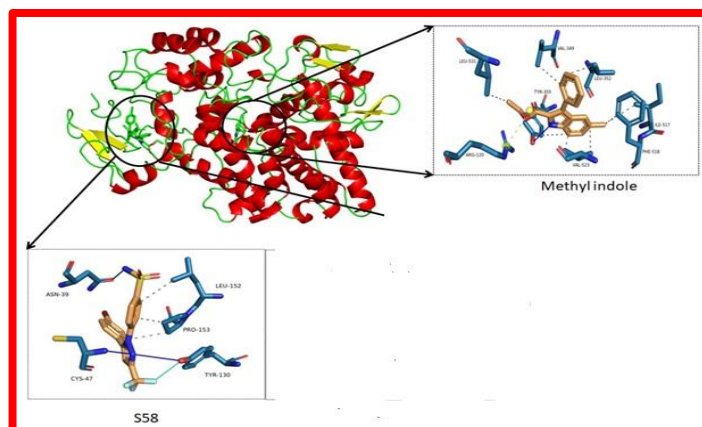| Comp.	BE (kcal/mol)	Inhibition constant	Hydrophobic Interactions	Hydrogen Bonds	Salt Bridges	pi-Stacking	Halogen Bonds
5-MPIC	-7.93	1.54uM	VAL349 LEU352 TYR355 ILE517 PHE518 VAL523 LEU531	TYR355	ARG120		
S58	-8.64	462.11nM	LEU152 PRO153	ASN39 CYS47 TYR130			TYR130

Figure-11: Three dimensional interaction of ligand in stick and aminoacids forming hydrogen interaction representation

4.2.7. a. Analysis of molecular lipophilicity potential (MLP)

MLP is calculated using atomic hydrophobicity contributions www.molinspiration.com. MLPs are

important properties that explain various molecular properties of ADME, such as membrane penetration and binding to plasma proteins. Hydrophobicity is indicated by purple and blue

coded levels and hydrophilicity by orange and red coded levels. It also shows how a particular molecule resembles a drug.
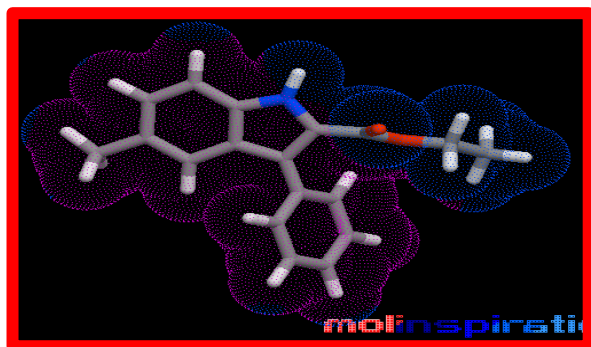

Figure 11: Molecular lipophilicity potential

Table-9. Bioactivity scores

GPCR ligand	-0.07
Enzyme inhibitor	-0.01
Protease inhibitor	-0.37
Nuclear receptor ligand	-0.01
Kinase inhibitor	0.03
Ion channel modulator	-0.14

b. Drug-likeness prediction

During lead development, molecules are compared to a set of criteria, including their ADMET scores, physicochemical properties, bioactivity scores and resemblance to other drugs. All of the synthesised compounds were put through an ADME (Absorption, Distribution, Metabolism, and Excretion) screening using the Swiss National Database (http://www.swissadme.ch/). The primary objective of this research is to make educated guesses about the pharmacokinetic properties of the compounds being studied. Newly synthesised compounds and their anticipated

ADMET features and drug-likeness profiles are shown in Table 10.

Table-10: Physiochemical parameters of compound predicted by Swiss ADME.

Parameters*	5-MPIC
MW	279.33
NHA	21
NAHA	15
NRB	4
NHBA	2
NHBD	1
MR	84.79
TPSA	42.09
i LOGp	3.03
Log S (ESOL)	-4.73
MLOGP	3.24
GI	High
BBBP	Yes
v LROF	0
v GR	0
v VR	0
BS	0.55
SA	2.61

- "Molecular weight=MW; Num. heavy atoms= NHA; Number of aromatic heavy atoms=NAHA; Num. rotatable bonds=NRB;: Num. H-bond acceptors-=NHBA; Num. H-bond donors= NHBD; Molar Refractivity=MR; Topological Polar Surface Area=TPSA; Solubility class=Log S; Moriguchioctanol-water partition coefficient = MLOGP; Gastrointestinal absorption =GI; Blood Brain Barrier Penetration=BBBP; Violation of Lipinski's rule of five=vLROF; Violation of Ghose rule= vGR; Violation of Veber rule=vVR; Bioavailability Score=BS; Synthetic accessibility =SA

Table 11: Statistical treatment of the spectral shift of the compound

Compound	Slope	R square	No of data
5-MPIC	m_1=18599	0.88	7
	m_2 = 5776	0.89	9
	m_3=-8545	0.88	7
	m = 8632	0.87	7

Table 12: Onsager radius, ground and excited state dipole moments of the compound

Compound	μ_e^h(D)	μ_e^g(D)	μ_e^f(D)	μ_e^e(D)	μ_e^d(D)	μ_e^c(D)	μ_g^b(D)	μ_g^a(D)	Radius(Å)
5-MPIC	5.17	5.46	6.76	5.43	11.1	6.77	1.30	0.88	3.730

(1Debye = 3.34×10^{-30}cm=10^{-18}esu cm.)"
[a]The ground state dipole moments using Gaussian software;
[b]The ground state dipole moment calculated using equation (10);
[c]The excited state dipole moment calculated using equation (11);

[d]The excited state dipole moment calculated from Lippert's equation (7);
[e]The excited state dipole moment calculated from Bakshieves equation (8);
[f]The excited state dipole moment calculated from Kawaski Chamma Viallets equation (9);

[g]The Change in dipole moment calculated using equation (10) and (11);

[h]Change in dipole calculated using equation (12).

Conclusion

We utilized solva tochromic shift technique to find out 5-MPIC's dipole moments in both excited as well as ground states by analysing emission and absorption spectra. As opposed to the dipole moment in ground state, excited state has a larger value. Since the polarity of excited state is much higher than ground state, dipole moment is also significantly elevated. The parameters of microscopic solvent polarity and solvatochromic shift were utilized for calculating the change in dipole moment and to make a comparison. Involvement of $\pi \rightarrow \pi^*$ transition was suggested by the solvatochromic shift measurements. Schiff bases in their excited and ground states were found to be very basic and acidic, respectively, by Catalan and Kamlet-Taft analyses. DFT /B3LYP employing the 6-31+G (d, p) basis set was utilized for optimising the geometry of target molecule. Internal charge transport was also calculated using HOMO-LUMO analysis. The Mulliken atomic charges provide light on the behaviour and reactivity of the molecules. As such, nonlinear optics (NLO) investigations of the provided chemical have potential practical uses. From the NBO analysis, π (C10-C11) $\rightarrow \pi^*$C29-030) has the highest stabilization energy of 26.93 Kj/mol. This confirms the ICT and thus supports the experimental evidence. Molecular docking study revealed that the indole derivative showed the most suitable binding pattern at the active site through interaction with cyclooxygenease-2.

References:

1. Onsager, L, Electric moments of molecule in liquid. J. Am. Chem. Soc. 1936,58, 1486-1493.
2. McRae, E.G. Theory of solvents influence on the molecular electronic spectra. Frequency shifted J. Phys. Chem 1957,61, 562-57.
3. Bakshieves N.G. Spectroscopy of inte rmolecular interaction; Nauka: St. Petersburg, Russian, 1972.
4. Abe T. Theory of solvent influence on the molecular electronic spectra. Frequency shifts. Bull. Chem. Soc.Jpn.1965, 38,1314-1318.
5. J.R. Lakowicz, Principle of Fluorescence Spectroscopy, Plenum Press, New York, 1983.
6. Zhang, Xue-Hua and Cui, Yan & Katoh, Ryuzi & Koumura, Nagatoshi & Hara, Kohjiro. (2010). Organic Dyes Containing Thieno[3,2-b] indole Donor for Efficient Dye-Sensitized Solar Cells. The Journal of Physical Chemistry C. 114. 10.1021/jp105548u.
7. B.S. Mathada, N.G. Yernale, J.N. Basha, J. Badiger, an insight into the advancd synthetic recipes to access ubiquitous indole heterocycles. Tetraheron Letter, Volume 85, 2021, 153458, https://doi.org/10.1016/j.tetlet.2021.153458.
8. N. G. Yernale, B. S. Mathad, G. B. Vibhutimath V, D. Biradar, M. R. Karekal, M. D. Udaygiri, M. B. Hiremathad , Indole core based Copper(II), Cobalt(II), Nickel(II) and Zinc(II) Complexes: Synthesis, spectral and biological Study, journal of Molecular structure, Volume 1248, 2022, 1311410, https://doi.org/10.1016/j.molstruc.2021.131410.
9. N.G. Yernale, B.H.M. Mruthyunjayaswamy, Metal (II) Complexes of ONO donor Schiff base ligand as a new class of bioactive compound containing indole core: Synthesis and characterization, Int JPharm Pharm Sci Vol8, Issue 1,197-204 (2016).
10. M. Sathisa, L, Rajasekaranb, D. Shanthi C, N. Kangathara d, S. Sarala e, S. Muthub, Journal of Molecular structure 2022.
11. Gümüş, Ayşegül and Gumus, Selcuk. (2022). Synthesis of Quinoline-Pyrene Derivatives and Theoretical Investigation of Their Fluore-scence and Electronic Properties. Chemistry Select. 7. 10.1002/slct.202203958.
12. Kawski, A. and Kukliński, B. and Bojarski, P. (2009). Photophysical properties and thermochromic shifts of electronic spectra of Nile Red in selected solvents. Excited states dipole moments. Chemical Physics. 359. 58-64. 10.1016/j.chemphys.2009.03.006.
13. Basavaraj, Shivaleela and Gounhalli, Shivraj & Patil, Omnath and Hanagodimath, S M Hanagodimath. (2021). Quenching of fluorescence, dipole moments and DFT studies of newly synthesized amino-thiadiazole coumarin derivative. 55. 200-218.
14. P K, Ingalagondi and Patil, Omnath and Shivaraj, G. and Sankarappa, T. and Hanagodimath, S M Hanagodimath. (2019). Solvent effect on the spectral properties of coumarin laser dye: Estimation of ground and excited state dipole moments. AIP Conference Proceedings. 2142. 140028. 10.1063/1.5122541.
15. Patil, Omnath and Hanagodimath, S M Hanagodimath. (2018). Estimation of ground and excited state dipole moments of newly synthesized coumarin (4-MPMHC) derivative.

16. Mathapati, G.B. and P K, Ingalagondi and Patil, Omnath and Basavaraj, Shivaleela and Gounalli, Shivaraj and Hanagodimath, S.M. (2019). Estimation of ground and excited state dipole moments of newly synthesized coumarin molecule by Solvatochromic shift method and Gaussian software. International Journal of Scientific Research in Physics and Applied Sciences. 7. 38-43. 10.26438/ijsrpas/v7i2.3843.

17. V.R. Desai, A.H. Sinargi, S.M. Hungund, M. Basangouda, R.M. Melavanki,R.H. Fattepur, J.S adadeavar math. J. Mol.Liq.,223(2016)141-149.

18. Koppal, Varsha & Patil, P.G. & Melavanki, R. & Patil, N.. (2018). Study on Solvent Effect and Estimation of Dipole Moments of Laser Dye 3ADHC. Materials Today: Proceedings. 5. 2759-2764. 10.1016/j.matpr.2018.01.062.

19. Kalpana Sharma, Raveendra Melavanki, S.S. Patil, R.A. Kusunur, N.R. Patil, V.M. Sher.J. Mol.Struc, 1181(2019)474-487.

20. S.P. Hiremath, B.H.M. Mrutyunjayaswamy, M.G. Purohit, Synthesis of substituted 2-aminoindoles and 2-(2'-phenyl-1',3',4'-oxadiazolyl aminoindole, IndianJournal0f Chemistry B,1978,16,9,789-792.

21. Mahadev Dhanraj Udayagiri, Nagesh Gunvanthrao Yernale, Bennikallu Hire Mathada Mruthyunjayaswamy, Int J Pharm Pharm Sci, Vol 8 (3), 2016, 344-351.

22. Mahadev Dhanraj Udayagiri, Nagesh Gunvanthrao Yernale, Bennikallu Hire Mathada Mruthyunjaya swamy, Der Pharma Chemica, 2016, 8(10):37-46.

23. E. Lippert, Z, Elektrocehm.,61(1957)962-975.

24. N.G. Bakshiev, Opt Spectrosk.,16(1964)821-832.

25. L.A.Kawski,Z.Naturforsch.,18a(1963)10256, Biolt.A.Kawski.,Naturforsch.,17A (1962)-621-627.

26. Chamma, p. Viallet, C.R. Acad, Sci.Paris Ser.C,270(1970)1901-1904.

27. J. T. Edward, Molecular Volumes and Parachor. Chem. Ind, London, pp. **774** (1956).

28. C.Reicardt, Solvents and solvent Effects in Organic Chemistry,2nd., VCH,1988.

29. Kamlet MJ, Abbound JM, Taft RW (1981) Progress in Physical Organic Chemistry. Wiley, New york.

30. Mataga N, Kubata T(1970) Molecular interactions and electronic Spectra. Marcel Dekker New York.

31. Catalan J (1995) On the π * Solvent scale J Org Chem 60(25):8315-831.

32. Catalan J (1997) On the ET (30) π *, Py, S' and SPP empirical scales as descriptors of nonspecific solvent effects' Org J Org Chem 62(23): 8231-8234.

33. Taft Rw, Abbound JLM, Kamlet M (1981) Solvatochromic comparison method.20: Linear solvation energy relationship-12: The dδ term in the solvatochromic equation's Am Chem Soc 103(5):1080-1086.

34. Catalan J, Lopez V, Perez P, Villamil RM, Rodrigues JG (1995) Progress towards a generalised solvent polarity scale: The solvatochromism of 2-(dimethylamino)-7-nitrofluorene and its homomorph 2-fluoro-7-nitrofluorene. Liebigs Ann 2:241-252.

35. Kurumbail RG, Stevens AM, Gierse JK, McDonald JJ, Stegeman RA, Pak JY, Gildehaus D, Miyashiro JM, Penning TD, Seibert K, Isakson PC, Stallings WC. Structural basis for selective inhibition of cyclooxygenase-2 by anti-inflammatory agents. Nature. 1996 Dec 19-26;384 (6610): 644-8. doi: 10.1038/384644a0. Erratum in: Nature 1997 Feb 6;385(6616):555. PMID: 8967954.

36. Morris, Garrett M., Huey Ruth, William Lindstrom, Michel F. Sanner, Richard K. Belew, David S. Goodsell, and Arthur J. Olson. 2009. Software News and Updates AutoDock4 and AutoDockTools4: Automated Docking with Selective Receptor Flexibility. Journal of Computational Chemistry 30(16):2785–91.

37. O Boyle, Noel M., Michael Banck, Craig A. James, Chris Morley, Tim Vandermeersch, and Geoffrey R. Hutchison. 2011. Open Babel: An Open Chemical Toolbox. Journal of Chemin formatics 3(33):1–14.

38. Dallakyan S, Olson AJ. Small-molecule library screening by docking with PyRx. Methods Mol Biol. 2015; 1263:243-50. doi: 10.1007/978-1-4939-2269-7_19. PMID: 25618350.

39. Melissa F Adasme, Katja L Linnemann, Sarah Naomi Bolz, Florian Kaiser, Sebastian Salentin, V Joachim Haupt, Michael Schroeder, PLIP 2021: expanding the scope of the protein–ligand interaction profiler to DNA and RNA, Nucleic Acids Research, Volume 49, Issue W1, 2 July 2021, Pages W530–W534, https://doi.org/10.1093/nar/gkab294

40. Kirilova, Elena and Yanichev, Artur & Pučkins, Aleksandrs and Fleisher, Mendel & Belyakov, Sergey. (2018). Experimental and theoretical study on structure and spectroscopic properties of 2-bromo-3-N- (N', N'-dimethyl formamide) benzanthrone. Luminescence. 33. 10.1002/bio.3538.

Eur. Chem. Bull. **2023**, *12(Special Issue 5), 6704 - 6717*

6716

41. C. Chandrasekhar, H.R. Deepa, R. Melavanki, S. Mogurampelly, M. B., S. Y, J. Tipperudrappa, Quantum chemical and Solvatochromic studies of biological active 1,3,4-thiadiazol coumarin derivatives, Chemical Data Collections. 29 (2020) 100516. https://doi.org/10.1016/j.cdc.2020.100516

42. Patil, Omnath and P K, Ingalagondi and S M Hanagodimath. (2021). Estimation of Dipole Moments of New Coumarin Dye by Experimental and Theoretical Methods. Macromolecular Symposia. 400. 2100015. 10.1002/masy.202100015.

43. Patil, Omnath and P K, Ingalagondi & Gounhalli, Shivraj & Hanagodimath, S M Hanagodimath. (2019). Dipole moments and quenching of fluorescence of a new coumarin dye. Canadian Journal of Physics. 98. 10.1139/cjp-2019-0517.

44. P. Bhavya, Raveendra Melavanki, R.A, Kalpana Sharma, Raviraj Kusanur, N R Patil, J. Thipperudrappa, Exploring the spectral features and quantum chemical computations of a novel biologically active heterocyclic class of compound 2MEFPBA dye: Experimental and theoretical approach, Chemical Data Collections, Volume 19, 2019,

45. T. Abbaz, A. Bendjeddou, D. Villemin, Theoretical Analysis and Molecular Orbital studies of Sulphonamides Products with N-Alkylation and O-alkylation, Int. J. Adv. Eng. Res. Sci. 6 (2019) 91–101. https://doi.org/10.22161/ijaers.6.2.12.

Eur. Chem. Bull. **2023**, *12(Special Issue 5), 6704 - 6717*

6717